PCCP

Accepted Manuscript

ROYAL SOCIETY OF CHEMISTRY

www.rsc.org/pccp

Dynamic Article Links ►

Cite this: DOI: 10.1039/c0xx00000x

www.rsc.org/xxxxxx

ARTICLE TYPE

Dielectric, thermal and mechanical properties of zirconium silicate reinforced high density polyethylene composites for antenna applications

Jobin Varghese[a,b], Dinesh Raghavan Nair[c], Pezholil Mohanan[c] and Mailadil Thomas Sebastian[a,b*]

Received (in XXX, XXX) Xth XXXXXXXXX 20XX, Accepted Xth XXXXXXXXX 20XX

DOI: 10.1039/b000000x

Low cost and low dielectric loss zirconium silicate ($ZrSiO_4$) reinforced HDPE (high-density polyethylene) composite has been developed for antenna applications. The 0-3 type composite is prepared by dispersing $ZrSiO_4$ filler for various volume fraction (0.1 to 0.5) in HDPE matrix by melt mixing process. Composite shows good microwave dielectric properties with relative permittivity of 5.6 and dielectric loss of 0.003 at 5 GHz at the maximum filler loading of 0.5 volume fraction. The composite exhibits low water absorption, excellent thermal and mechanical properties. It shows a water absorption of 0.03 wt. %, coefficient of thermal expansion of 70 ppm/°C and room temperature thermal conductivity of 2.4 W/mK. The composite shows tensile strength of 22 MPa and microhardness of 13.9 Kg/mm^2 for the filler loading of 0.5 volume fraction. The HDPE-$ZrSiO_4$ composites show good dielectric, thermal and mechanical properties suitable for microwave soft substrate applications. A microstrip patch antenna is designed and fabricated using HDPE-0.5 volume fraction $ZrSiO_4$ substrate and investigated the antenna parameters.

Introduction

The recent rapid developments in the telecommunication industries, demand the requirement of high efficiency and low-cost composite materials which can considerably reduce the cost of consumer electronics. The cost aware product miniaturization has been the long demanding need of electronic industries. In this context, several ceramics such as silicates, phosphates and aluminates with excellent microwave dielectric, thermal and mechanical properties have been developed for substrate and packaging applications [1-3]. Many ceramics materials meet its dielectric and thermal properties, however, the production cost of the ceramics is high. The brittleness and high processing temperature of ceramics lead to the difficulty in fabrication of complex shapes or machining substrates during circuit fabrication. In order to compensate the cost and processing, ceramic substrates used in the microwave modules are widely replaced by cheaper polymer-ceramic composite substrates having reasonably good performance [4-7]. Many of the polymers satisfy the criteria of low relative permittivity (ε_r) and low dielectric loss tangent (tan δ) which are essential for substrate applications [8]. The major disadvantages of the polymers are their high value of the coefficient of thermal expansion and inferior thermal conductivity. A combination of polymers and ceramic fillers can effectively resolve the processing cost as well as processing difficulties with balanced dielectric, thermal and mechanical properties. An ideal substrate material should have low dielectric loss, optimum relative permittivity, high thermal conductivity, matching thermal expansion to that of conductor materials attached and good mechanical properties [9-12].

Extensive research work has been carried out in the area of polymer-ceramic composites for soft substrate applications [8]. Commonly used soft substrate materials are polytetrafluoroethylene (PTFE), epoxy, high-density polyethylene (HDPE), polystyrene (PS), etc. [8]. Among the various thermoplastics, HDPE is an easily processable polymer with excellent microwave dielectric properties (ε_r = 2.3, tan δ = ~ 10^{-4}) [13]. HDPE is a non-polar, semi-crystalline polymer composed of -CH_2-CH_2- monomer units [14] and easily remolded into various shapes. The other reason for using HDPE is to achieve solid waste reduction as well as the low cost. Recently HDPE filled with several ceramics such as CeO_2 [15], $Sm_2Si_2O_7$ [13], Li_2MgSiO_4 [16], $Sr_2ZnSi_2O_7$ [17], $Ca_4La_6(SiO_4)_4(PO_4)_2O_2$ [4], $Sr_2Al_2SiO_7$ [5] with relative permittivity up to about 7 and tan δ of the order of 10^{-3} in the microwave frequency range have been reported. All these composites have relatively low CTE in the range of 75-150 ppm/°C with good thermal conductivity and mechanical properties.

In the present paper, we report the dielectric, thermal and mechanical properties of HDPE polymer matrix filled with low cost $ZrSiO_4$ ceramic. $ZrSiO_4$ has excellent dielectric and thermal properties (ε_r = 9.1, Qu×f = 32,000 GHz at 10 GHz and TC = 15 W/mK, CTE = -2.5 ppm/°C) among the orthosilicates [18]. Moreover, $ZrSiO_4$ ceramic is an abundant mineral which reduces the production cost of soft substrates. Recently considerable attention has been paid for cost effective miniaturization of devices. In modern era, antennas are eyes and ears of the world which regulate the modern wireless communication. Low-cost low profile antennas are getting importance in areas such as high-performance aircrafts, spacecraft, satellites and missile technology [19, 20]. The present paper investigate the preparation, characterization and properties of HDPE-$ZrSiO_4$ ceramics for soft substrate applications. A microstrip patch antenna based on the newly developed soft substrate has been designed and fabricated.

Results and Discussion

Structural and microstructural analysis

Figure 1 (a) depicts the X-ray diffraction patterns of $ZrSiO_4$ ceramic, HDPE matrix and its composites. The peaks of $ZrSiO_4$ ceramic belong to the tetragonal crystal structure as evident from Figure 1 (a) [18]. The most crystalline forms of high-density polyethylene (HDPE) are solid orthorhombic, metastable monoclinic and high-pressure ortho hexagonal. Both orthorhombic and monoclinic phases have planar zigzag chain configuration. Orthorhombic phase has two distinct diffraction peaks at $2\theta = 21.4^o$ corresponding to the (100) plane with d_{100} = 0.42 nm and $2\theta = 23.65^o$ corresponding to (200) plane with d_{200} = 0.37 nm [21]. The XRD peaks observed at angles 21.4^o, and 23.65^o corresponds to orthorhombic structure of HDPE matrix. The volume fraction (V_f) of ceramic filler varied from 0.1 to 0.5 and Figure 1 (a) also represents the X-ray diffraction pattern of HDPE-$ZrSiO_4$ composites. The diffraction peaks of HDPE-$ZrSiO_4$ composites show good agreement to that of the diffraction pattern of HDPE matrix and $ZrSiO_4$ ceramic filler. The amount of HDPE in the composite materials under diffraction decreases as compared to $ZrSiO_4$. Hence the intensity of HDPE diffraction peak decreases and that of $ZrSiO_4$ increases. The X-ray intensity variation in the 0.5 V_f as compared to the lower filler loading may be due the instrumental error.

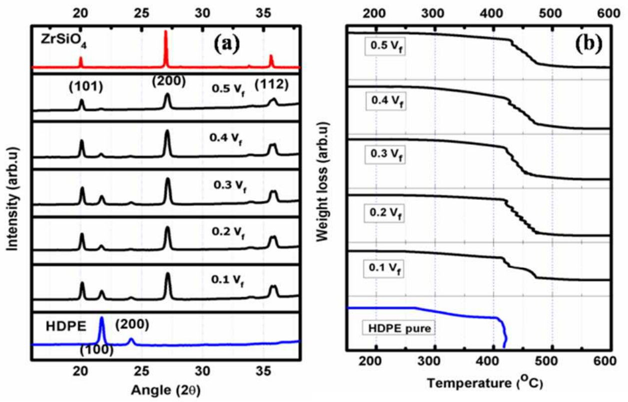

Fig. 1 (a) X-ray diffraction pattern $ZrSiO_4$ ceramic filler and (b) TGA curve of HDPE matrix and its composites at different volume fractions

Figure 1 (b) shows the thermogravimetric analysis (TGA) of HDPE-$ZrSiO_4$ composites. The beginning of decomposition is the same for pure and for all volume fractions of $ZrSiO_4$ fillers while ending is extended between 400-500 ^oC. The extended weight losses is due to the increase in filler loading. The TGA measurements of pure HDPE demonstrate that the weight loss starts at around 280 ^oC and become complete at around 400-450 ^oC. However, it has been reported that the thermal degradation of 99 wt. % polymer starts at 402.84 ^oC for pure HDPE and 420 ^oC for recycled HDPE [22]. The degradation temperature of pure HDPE is around 405 ^oC and it is increased by the addition of $ZrSiO_4$ filler with HDPE matrix. The complete degradation of HDPE-$ZrSiO_4$ composites completes at around 420 ^oC as shown in Figure 1 (b). The total weight losses for each V_f of filler in the HDPE-$ZrSiO_4$ composites are shown in Figure 1 (b).

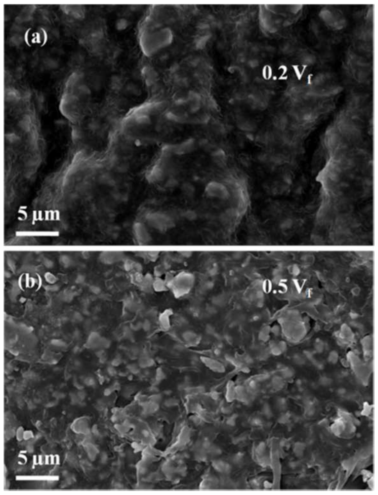

Fig. 2 SEM images of HDPE-$ZrSiO_4$ composites with (a) 0.2 V_f and (b) 0.5 V_f of $ZrSiO_4$

Figures 2 (a) and (b) respectively show the SEM images of the HDPE-$ZrSiO_4$ composite loaded with 0.2 V_f and 0.5 V_f of $ZrSiO_4$ ceramic filler. Figure 2 (a) shows that most of the filler particles remain isolated from each other in the polymer matrix in HDPE-0.2 V_f $ZrSiO_4$ composite. On the other hand, for the highest filler loading of 0.5 V_f the inter-particle distance decreases and filler particles tend to agglomerate as evident from Figure 2 (b). The connectivity among the ceramic particles increases for higher mixing ratios that in turn improves the properties. The matrix filler connectivity of the composite is important since it controls the electric flux pattern as well as mechanical and thermal properties [23]. For polymer-ceramic composites, there is a maximum limit of filler loading above which the processing becomes difficult and also results in poor mechanical properties [24]. In HDPE-$ZrSiO_4$ composites, the highest filler loading achieved is 0.5 V_f. The increase in the porosity of the composite with the rise in volume fraction of $ZrSiO_4$ leads to the aggregation of the ceramic particles in the continuous HDPE matrix.

Density, water absorption and dielectric properties of the composites

Table 1 shows the relative density, water absorption and dielectric properties at 1 MHz and 5 GHz. From the Table 1 it is clear that the density of the composite increases with an increase in filler volume fraction which is due to the higher density of the $ZrSiO_4$. In composite materials, water absorption will lead to the overall degradation of dielectric properties both at radio and microwave frequencies [13, 25, 26]. The absorbed water acts as an interlayer between the polymer matrix and ceramic filler which in turn causes an interfacial loss mechanism at low frequencies [27]. The dipole relaxation of absorbed water may also produce additional loss at microwave frequencies [12]. In addition to this, the vaporization of absorbed water due to the heat generated during soldering may lead to delamination and crack of the soft substrate [28]. Moisture absorption of less than 0.1 % has been reported to be ideal for electronic packaging applications [29]. From Table 1, it is evident that HDPE-$ZrSiO_4$ composites show negligible tendency for water absorption ranging from 0.02-0.03 wt. % for the composites with its filler loading ($V_f = 0.1$ to 0.5). The relative permittivity (ε_r) of HDPE-$ZrSiO_4$ composites at 1 MHz increases gradually with filler volume fraction (Table 1) due to relatively large relative permittivity of the $ZrSiO_4$ filler compared to HDPE matrix. It increases from 3.1 to 6 for the filler V_f from 0.1 to 0.5 at a frequency of 1 MHz. The dipole-dipole interaction increases with an increase in filler loading, and it also contributes to higher relative permittivity as $ZrSiO_4$ fillers come closer at higher filler loading. In addition to this, the Maxwell-Wagner-Sillars effect appears in heterogeneous media due to the accumulation of charges at the interface that leads to the formation of large dipoles [30]. The dielectric loss tangent (tan δ) at 1 MHz increases from 0.0007 for 0.1 V_f $ZrSiO_4$ to 0.002 for 0.5 V_f $ZrSiO_4$ in HDPE matrix. The decrease in the homogeneity with filler loading leads to increase in dielectric loss tangent [31].

Table 1 Density, water absorption and dielectric properties at 1 MHz and 5 GHz of HDPE-$ZrSiO_4$ composites

V_f of filler	Density (g/cm^3)	Water absorption (wt. %)	At 1 MHz		At 5 GHz	
			ε_r	tan δ	ε_r	tan δ
0.1	1.33	0.02	3.1	0.0007	2.9	0.0008
0.2	1.70	0.02	3.9	0.0008	3.5	0.0009
0.3	2.08	0.02	4.6	0.0009	4.0	0.0012
0.4	2.45	0.03	5.3	0.0010	4.8	0.0018
0.5	2.83	0.03	6.0	0.0020	5.6	0.003

The variation of both relative permittivity and dielectric loss tangent at 5 GHz with volume fraction of filler follows a similar trend as that observed at 1 MHz. The relative permittivity of the composite at microwave frequency is smaller as compared to 1 MHz and is due to the difference in the polarization mechanisms. The composite with maximum filler loading of 0.5 V_f $ZrSiO_4$ has ε_r of 5.6 and tan δ of 0.003. In polyethylene, the significant aid towards dielectric loss come from branching, vinyl unsaturation, and impurity dipolar structures introduced while processing [32, 33]. The dielectric loss tangent is the primary factor affecting frequency selectivity of materials. The factors such as anharmonic interaction of the electric field with the phonon system, imperfections in a crystal lattice, order-disorder and impurities influence the loss tangent [1]. Consider the composite as a whole, additional effects arising from heterogeneity, porosity, and matrix-filler interphase region may also can affect the loss factor [31, 34, 35].

Figure 3 (a) depicts the comparison of the experimentally observed values of relative permittivity at 5 GHz with the theoretical predictions for HDPE-$ZrSiO_4$ composites. The theoretical values of relative permittivity predicted using Lichtenecker [36, 37], Modified Lichtenecker [29, 38], Maxwell Wagner [39], EMT [40] and Jayasundere-Smith [41] models are compared with experimental results. The Lichtenecker model shows a wide deviation from the experimental values even for low filler loadings. Lichtenecker model describes the composite system as a continuous matrix with randomly oriented spheroids. This model does not provide an appropriate match to the experimentally observed values of relative permittivity for HDPE-$ZrSiO_4$. Conventional mixing rule and Lichtenecker model does not explain the filler matrix interactions. The modified Lichtenecker equation describes the filler matrix interaction by introducing a correction term. However, modified Lichtenecker model also shows considerable variation in the experimental and theoretical values and may be due to the deviation of its principle to the developed composites. In addition to this, the values of relative permittivity obtained using Maxwell-Wagner and EMT model shows considerable difference between the experimentally observed values especially at higher filler loading (Figure 3 (a)). The values of relative permittivity obtained using Jayasundere-Smith is found to be matching with the experimental data (Figure 3 (a)). This model assumed a bi-phase system consisting of dielectric spheres dispersed in a continuous medium of matrix and hence is suitable for both lower and higher filler loading. However, the effective permittivity will depend on the permittivity of each phase in the mixture, volume fraction, shape and size of the filler particle, porosity and interface between the matrix and filler [36]. The aging of microwave dielectric properties of HDPE-$ZrSiO_4$ composite is important for practical applications. Figure 3 (b) depicts the effect of shelf life on microwave dielectric properties of developed HDPE-$ZrSiO_4$ composites at 5 GHz. From the Figure 3 (b) it is evident that over a period of one year, relative permittivity and dielectric loss tangent of HDPE-$ZrSiO_4$ composites exhibit only a marginal deviation and is within the error limit of SPDR (Split Post Dielectric Resonator) measurement. The variation in the dielectric loss of 0.1 V_f after 2 month of measurement may be due the atmospheric humidity and moisture absorption within the sample [1].

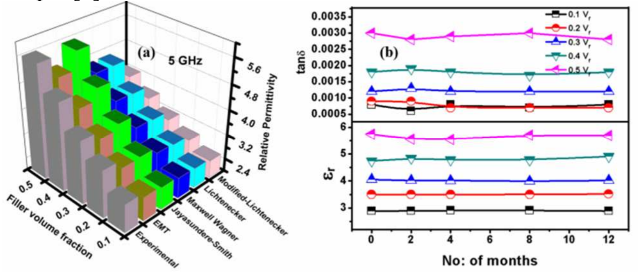

Fig. 3 (a) Comparison of experimental and theoretical relative permittivity and (b) Effect of aging on microwave dielectric properties of HDPE-$ZrSiO_4$ at 5GHz.

Thermal and mechanical properties

Figure 4 (i) shows the comparison of experimental and theoretically predicted thermal conductivity of HDPE-$ZrSiO_4$ composites using theoretical models such as series [42, 43], geometric mean [44], Maxwell-Eucken [45-47], Agari [48, 49] and Cheng-Vachon [50]. For HDPE-$ZrSiO_4$ composites, thermal conductivity increases with an increase in filler loading due to the high thermal conductivity of $ZrSiO_4$ ceramic filler (15 W/mK) compared to HDPE matrix. The thermal conductivity of HDPE-$ZrSiO_4$ composite increases from 0.45 W/mK of pure HDPE to 0.74 and 2.3 W/mK respectively for 0.1 and 0.5 V_f of $ZrSiO_4$ in HDPE matrix. This may be due to the presence of more connecting paths between filler particles without disturbing the matrix. A similar observation of variation in thermal conductivity was reported by Kim et al. in AlN-epoxy composites [51]. The experimental results of HDPE-$ZrSiO_4$ composites are close to the predictions of Chen-Vachon as well as Geometric mean model. Increase in the volume fraction of $ZrSiO_4$ results in the agglomeration of ceramic particles as seen from SEM images shown in Figure 2 (a, b), thereby increasing the mismatch between the experimental and theoretical values. The predicted thermal conductivity using Maxwell-Eucken, series mixing and Agari model holds matching thermal conductivity at lower filler loading, and these models deviate from the experimental results for higher filler loading.

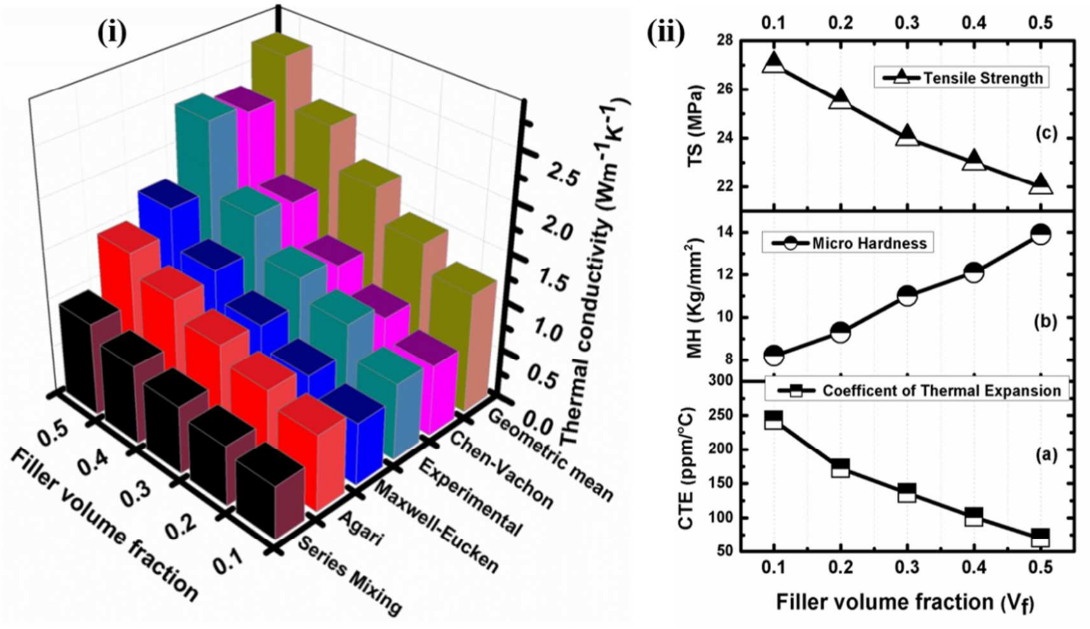

Fig. 4 (i) Experimental and theoretical thermal conductivity and (ii) Variation of (a) linear coefficient of thermal expansion, (b) microhardness and (c) tensile strength with filler volume fraction of HDPE-$ZrSiO_4$ composites

The Maxwell-Eucken model predicts values significantly below experimental data of HDPE-$ZrSiO_4$ composites, and this is because it does not account for differences in morphology as well as the effects of chain formation. Theoretical models account for variations in the size, shape, intrinsic thermal conductivity and state of dispersion of the filler. The wide variation in filler geometry, orientation and distribution makes it difficult to predict the thermal conductivity of the composites with finite accuracy. The theoretical models do not account the porosity of the composites. As a result, experimental and theoretical thermal conductivity data are often not in agreement especially at higher filler loadings [52].

Figure 4 (ii) (a) shows the variation of the linear coefficient of thermal expansion (CTE) of HDPE- $ZrSiO_4$ composites with filler volume fraction. The CTE value decreases gradually with an increase in filler volume fraction and is due to the very low CTE value possessed by the $ZrSiO_4$ filler as compared to the polymer matrix. It is evident from the figure that CTE decreases almost linearly from 243 ppm/^{o}C to 70 ppm/^{o}C as the filler loading increases from 0.1 to 0.5 V_f. This is due to the higher CTE of HDPE matrix (250 ppm/^{o}C) [13] than that of $ZrSiO_4$ filler (-2.5 ppm/^{o}C) [18]. During heating of the composites, the polymer matrix will undergo more expansion as compared to ceramic fillers. However, the matrix- filler inter-phases are able to transmit the thermal stress, and the expansion of the matrix will get reduced. The CTE of the matrix will be lowered, if the interfaces between matrix and filler are capable of transmitting the stress developed [53, 54]. In HDPE-$ZrSiO_4$ composites, the linear decrease in CTE with filler volume fraction indicates that the matrix-filler adhesion is good enough to withstand the thermal stress.

Microhardness testing with a point indenter is a simple way to measure the mechanical properties of the soft substrates. Figure 4 (ii) (b) shows the variation of microhardness of HDPE matrix composites with $ZrSiO_4$ ceramic filler addition. Microhardness of $ZrSiO_4$ is reported to be in the range of 800-1200 Kg/mm^2 [55] while pure HDPE matrix has only 7 Kg/mm^2. As the volume fraction of $ZrSiO_4$ increases, the hardness of HDPE-$ZrSiO_4$ composites also increases. Microhardness increases from 8.2 to 13.9 Kg/mm^2 for the variation in the filler loading from 0.1 to 0.5 V_f with a standard deviation of 0.45. Figure 4 (ii) (c) shows the variation of tensile strength of the HDPE-$ZrSiO_4$ composites with filler loading. Tensile strength decreases from 27 MPa to 22 MPa as the filler concentration increases from 0.1 to 0.5 V_f. The mechanical strength of HDPE is mainly due to its semi-crystalline structure and is evident from the orthorhombic structure of HDPE matrix indicated in the structural analysis (Figure 1 (a)). When the polymers are loaded with more and more inorganic fillers, the deformation area in the matrix decreases which in turn reduces the tensile strength [56]. Moreover, the increase in porosity with filler loading may also bring about a reduction in tensile strength as the presence of air in the composites weakens the filler-matrix interface [57]. Weak interface is one of the reasons for reduced tensile strength. The interface volume increases at higher filler loading which leads to more filler-filler interaction and hence weakens the filler-matrix interface of the composite.

Design, fabrication and characterization of microstrip patch antenna

A microstrip patch antenna is designed and fabricated using HDPE-0.5 V_f $ZrSiO_4$ substrate. The patch has length L2 = 47 mm, breadth B2 = 46 mm, and substrate thickness T2 = 0.64 mm and relative permittivity of 5.6. The designed patch is excited by using proximity coupled feeding. Figure 5 (a) shows the designed geometry of the patch antenna and corresponding design parameters listed out in the Table 2. The proximity coupled feeding is designed and fabricated using FR4 substrate having relative permittivity of 4.4 and thickness (T1) 1.65 mm. This feeding technique has following advantages, easy to model, high bandwidth and low spurious radiations as compared to other feeding techniques [58]. In this case, the patch antenna radiates due to the fringing fields between underneath of the patch and the ground plane [59].

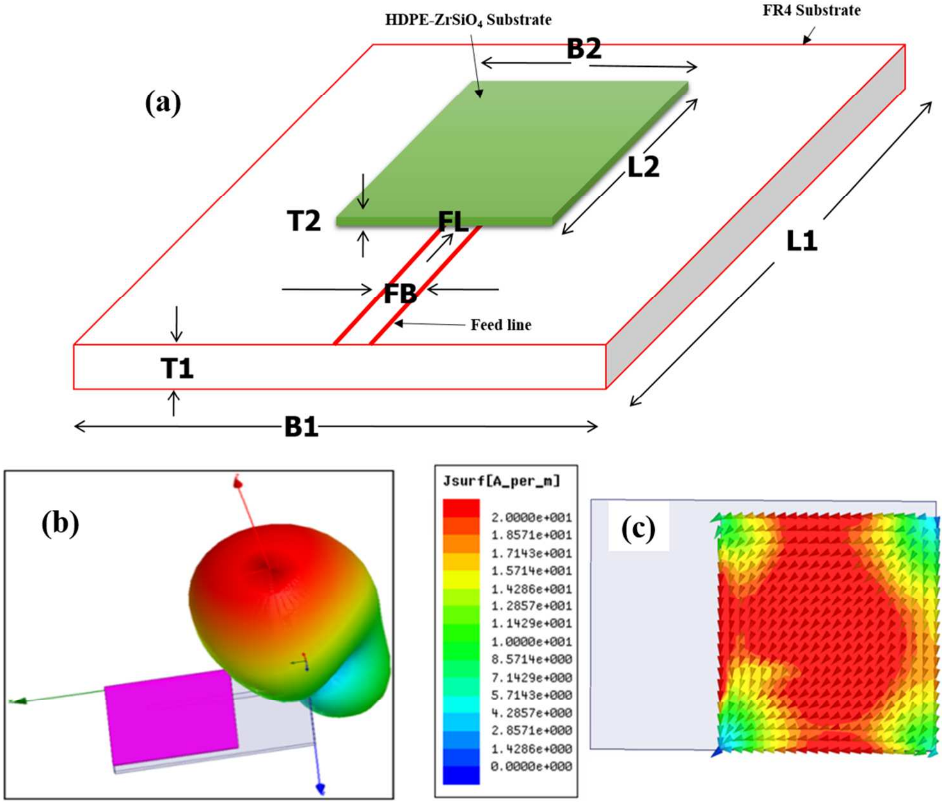

Fig. 5 (a) Design of microstrip patch antenna using proximity coupled feeding, (b) 3D radiation pattern and (c)Surface current distribution of simulated microstrip path antenna.

The designed antenna shows semicircular radiation pattern at 1.64 GHz, and simulations show return loss of -22 dB for HDPE-(0.5 V_f) $ZrSiO_4$. Figure 5 (b) (c) shows the 3D and 2D surface current distribution of unidirectional microstrip patch antenna. The 3D surface current distribution plot gives the relationship between the co-polarization and cross-polarization components (Figure 5 (b)). Moreover, it gives a clear picture of the nature of polarization of the fields propagating through the patch antenna. Figure 5 (b and c) clearly shows the linearly polarized microstrip patch antenna.

Figure 6 (a) depicts the simulated and measured return loss of microstrip patch antenna based on HDPE-$ZrSiO_4$ substrate. Fabricated prototype of the microstrip patch antenna is depicted in the inset of the Figure 6 (a). In the present case, antenna resonates at 1.64 GHz with return loss of about -24 dB, and it shows an excellent match with simulated results of HDPE-$ZrSiO_4$ soft substrate based microstrip patch antenna. A comparison of normalized radiation patterns for the E-plane and H-plane are shown in the figure 6 (b).

Table 2 Design parameters of designed antenna

Antenna design parameters	Dimensions (mm)
Length (L1) FR4 substrate	75
Breadth (B1) FR4 substrate	49
Thickness (T1) FR4 substrate	1.65
Length (L2) HDPE+$ZrSiO_4$ substrate	47
Breadth (B2) HDPE+$ZrSiO_4$ substrate	46
Thickness (T2) HDPE+$ZrSiO_4$ substrate	0.64
Feed Length (FL)	60
Feed Breadth (FB)	3

The E-plane is indicated in the figure by the top view of the microstrip patch antenna and is parallel to the feed line while H-plane lays perpendicular to the feed line [60-62]. The measured radiation patterns of the present antenna (Figure 6 (b)) shows a similar trend as that of a rectangular microstrip patch antenna.

The results shows that the developed soft substrates are suitable for the cost effective fabrication of microstrip antenna applications.

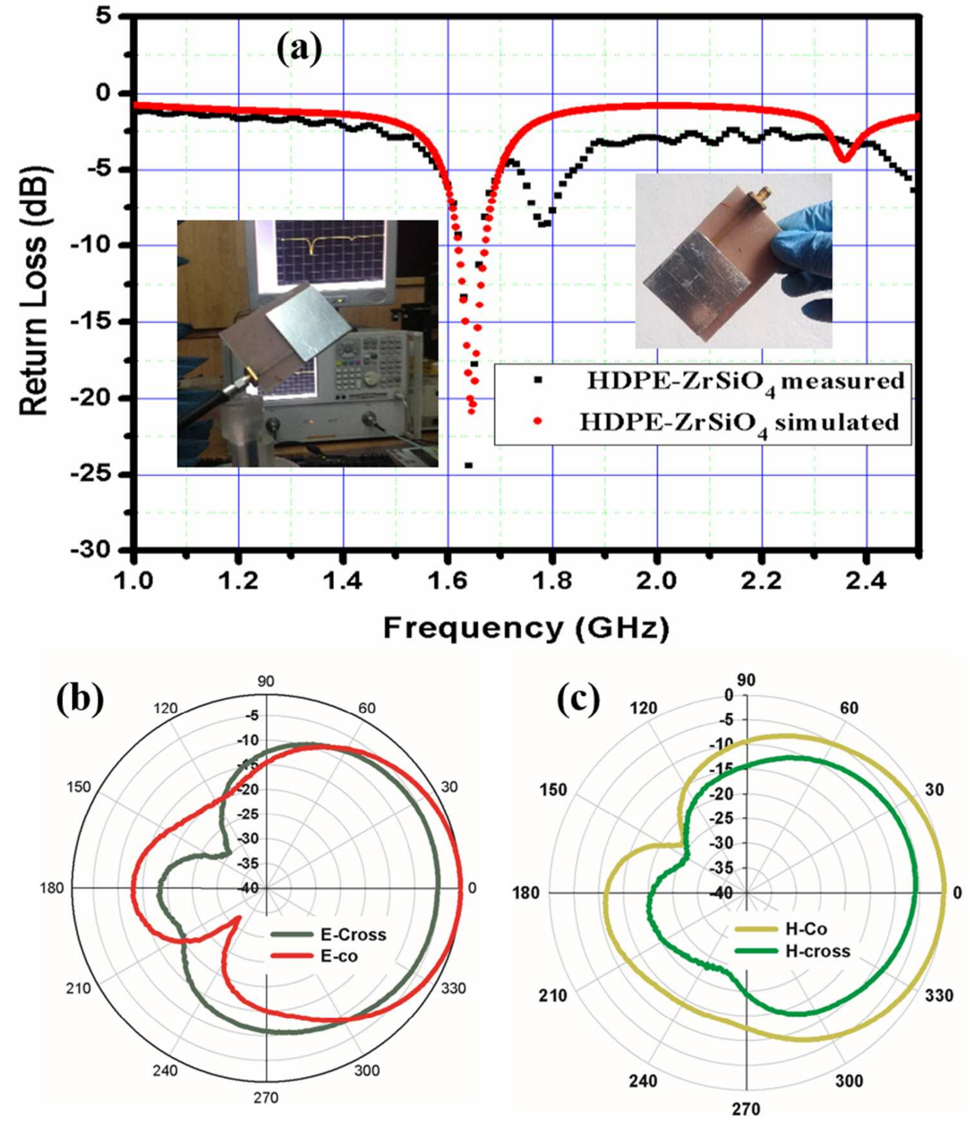

Fig. 6 (a) Simulated and measured return loss and radiation patterns of (b) E-plane and (c) H-plane of microstrip patch antenna based on HDPE-$ZrSiO_4$ substrate.

Experimental Section

Commercially available $ZrSiO_4$ powder was purchased from Sigma-Aldrich (98 %,St. Louis, MO-63103 USA). The powder obtained was pre-heated at 1000 ^{o}C and then calcined at 1400 ^{o}C for 4 hours with intermediate grinding. Calcined powder was ground and sieved through 25 µm sieve. The kneading machine at a temperature of 180 ^{o}C was used to prepare the composite by melt mixing different volume fractions (V_f) of $ZrSiO_4$ filler into HDPE (Nikunj Industries, Mumbai, India) matrix. The obtained mixtures were then hot pressed at 180 ^{o}C for 30 minutes under a pressure of 20 MPa. The phase formation of the ceramic filler and HDPE-ceramic composites was identified by recording X-ray diffraction pattern with CuKα radiation (X'Pert PRO MPD X-ray diffractometer, PANalytical, Almelo, Netherlands). Thermogravimetric analysis of HDPE-$ZrSiO_4$ composites was performed to determine the decomposition temperature of the developed composites. The bulk densities of the composites were measured by the Archimedes method. The microstructure of the composites was studied using Scanning Electron Microscope (SEM) (JEOL JSM-5600LV, Tokyo, Japan). Water absorption characteristics of the composites were measured using samples with dimensions 50 × 50 × 2 mm. The dielectric properties at 1 MHz were measured by parallel plate capacitor method using an LCR meter (Hioki 3532-50 LCR HiTESTER, Nagano, Japan). The error associated with the LCR measurement of relative permittivity and dielectric loss is < ±2 % [63]. Microwave dielectric properties were measured by Split Post Dielectric Resonator (SPDR) (QWED, Warsaw, Poland) method operated at 5 GHz using a Vector Network Analyzer (E5071C, Agilent Technologies, Santa Clara, CA). Using SPDR technique the total uncertainty of real permittivity does not exceed 0.5 % and is possible to resolve dielectric loss tangents to approximately 5 × 10^{-5} [64]. The linear coefficient of thermal expansion of the composites measured in the temperature range of 30-100 ^{o}C using a dilatometer (NETZSCH, Model DIL 402 PC, Germany) with accuracy < 1 %. The thermal conductivity of the composites was measured using Laser Flash technique (Anter Corporation, Flashline 2000, Pittsburgh, PA). The tensile test of the composites was conducted using dumb-bell shaped samples of width 4 mm and thickness 2 mm in a Universal Testing Machine (UTM, Hounsfield, H5K-S UTM, Redhill, UK). Microhardness of the developed composites was measured using Vickers hardness tester (Clemex 4, Germany). Effect of aging on microwave dielectric properties of the developed substrates was studied by measuring its dielectric properties for a period of one year.

A microstrip patch antenna was designed by simulations using Ansoft HFSS (high frequency structure simulator). A prototype of microstrip patch antenna was designed and fabricated on the developed soft substrates having relative permittivity of 5.6 (HDPE-$ZrSiO_4$ soft substrate) with thickness 0.64 mm. The proximity coupled feed made on FR4 substrate was used to feed the antenna. The antennas were designed and fabricated using conductive silver tape stick on the developed substrates placed in proximity coupled feed made with FR4 substrates. The fabricated antenna is characterized using HP8510C vector network analyzer and radiation characteristics were measured in anechoic chamber.

Conclusion

Low-cost microwave soft substrate is developed by reinforcing $ZrSiO_4$ ceramic in HDPE matrix. The composites show good density, low water absorption and good microwave dielectric properties. The composite with the highest filler content of 0.5 V_f showed ε_r of 5.6 and tan δ of 0.003 at 5 GHz with low water absorption of 0.03 wt. %. The relative permittivity of the composite is found to be in agreement with, Jayasundere-Smith model while thermal conductivity with Geometric mean and Chen-Vachon models. The HDPE-$ZrSiO_4$ composite shows, room temperature thermal conductivity of 2.4 W/mK for the maximum filler loading of 0.5 V_f. The CTE decreases with filler loading and a minimum CTE of 70 ppm/^{o}C is attained by the composite at maximum filler loading. The tensile strength of the composites also decreases slightly and reaches 22 MPa at 0.5 V_f of $ZrSiO_4$ in HDPE matrix. On the other hand, microhardness of the developed substrates shows an increasing trend and reaches around 14 Kg/mm^2 at its maximum filler loading. HDPE-$ZrSiO_4$ composites show excellent dielectric and thermal properties suitable for soft substrate applications. The microstrip patch antenna based on HDPE-$ZrSiO_4$ ($V_f = 0.5$) substrate is designed by using proximity coupled microstrip feed and a prototype is fabricated and tested. A prototype of microstrip patch antenna has been developed by using HDPE-$ZrSiO_4$ ($V_f = 0.5$) substrate. The developed microstrip patch antenna resonates at 1.64 GHz with return loss of -24 dB. The simulated and measured results show excellent agreement, and this substrate is a suitable candidate for antenna applications.

Acknowledgements

One of the author Jobin Varghese acknowledges to CSIR, New Delhi for the financial support.

Notes and References

[a] *Functional Materials, Materials Science and Technology Division, CSIR-NIIST,, Thiruvananthapuram, Kerala, India; E-mail: mailadils@yahoo.com*

[b] *Department of Electrical Engineering, Microelectronics and Materials Physics Laboratory, University of* Oulu, FI90014 Finland.

[c] *Department of Electronics, Cochin University of Science and Technology, Cochin 682022, Kerala, India.*

1. M. T. Sebastian, *Dielectric materials for wireless communications*, Elseiver Science and Technology Publishers, Oxford, U.K, 2008.
2. N. M. Alford, J. D. Brichall, K. Kendall, *Article of ceramic material and production therof*, US Patent: US5248464A, 1993.
3. S. Tomonori, T. Tsutomu, K. Ken-ichi, H. Ohsato, *J. Eur. Cerm. Soc.* 2006, 26, 2097.
4. D. Thomas and M. T. Sebastian, *J. Electron. Packaging*, 2014, 136, 031002.
5. K. M. Manu, S. Ananthakumar and M. T. Sebastian. *Ceram. Int.,* 2013, 39, 4945.
6. S. Rajesh, K. P. Murali, R. Ratheesh, *Appl. Phy. A*, 2011, 104, 159.
7. M. Teirikangas, J. Juuti and H. Jantunen,*Prog. Electromagn. Res.*, 2011, 115, 147.
8. M. T. Sebastian and H. Jantunen, *Int. J. Appl. Ceram. Technol.,* 2010, 7, 415.
9. R. Tummala, M. Kosec, W. K. Jones, and D. Belavic, *Electronic packaging for high reliability; low cost electronics*, Kluwer Academic Publishers, Dordrecht, The Netherlands, 1999.
10. D. D. L. Chung,*Polym. Polym. Compos.,* 2000, 8, 219.
11. N. K. James, P.S. Simna, R. Ratheesh, *Int. J. Materials and Structure Integrity*, 2013, 7, 22.
12. F. Xiang, H. Wang and X. Yao, *J. Eur. Ceram. Soc.,* 2006, 26, 1999.
13. S. Thomas, V. Deepu, S. Uma, P. Mohanan, J. Philip and M. T. Sebastian, *Mater. Sci. Eng. B*, 2009, 163, 67.
14. A. J. Bur, *Polymer*, 1985, 26, 963.
15. P. S. Anjana, V. Deepu, S. Uma, P. Mohanan, J. Philip and M. T. Sebastian, *J. Polym. Sci. B: Polym. Phys.*, 2010, 48, 998.
16. S. George, P. S. Anjana, M. T. Sebastian, J. Krupka, S. Uma and J. Philip, *Int. J. Appl. Ceram. Technol.*, 2010, 7, 461.
17. T. Joseph, S. Uma, J. Philip andM. T. Sebastian, *J. Mater. Sci.: Mater. Electron.*, 2012, 23, 1243.
18. J. Varghese, T. Joseph and M.T. Sebastian, *Mater. Lett.*, 2012, 65, 1092.
19. D. Guha, S. Chattopadhya and J. Y. Siddiqu, *IEEE Antennas Propagat. Mag.*, 2010, 52, 92.
20. D. Sarmah, N. S. Bhattacharyya and S. Bhattacharyya, *IEEE Trans. Dielectr. Electr. Insul.*, 2013, 20, 1845.
21. H. Huang, *Chin. J. Polym. Sci.*, 2000, 18, 363.
22. S. Oza, R. Wang, N. Lu, Intr. *J. Appl. Sci. Tech.*, 2011, 1, 31.
23. S. D. Malachlan, M. Blaskiewicz, and R. E. Newham, *J. Am. Ceram. Soc.*, 1990, 73, 2187.
24. J. W. Xu, K. S. Moon, C. Tison and C. P. Wong, *IEEE Trans. Adv. Packag.*, 2006, 29, 295.
25. R. F. Field, *J. Appl. Phys.*, 1946, 17, 318.
26. W. R. Tinga, W. A. G. Voss and D. F. Blossey, *J. Appl. Phys.*, 1973, 44, 3897.
27. P. A. M. Steeman, F. H. J. Maurer and M. A. van Es, *Polymer*, 1991, 32, 523.
28. M. Amagai,*Microelectron. Reliab.*, 2002, 42, 607.

29. S. Rajesh, V. S. Nisa, K. P. Murali and R. Ratheesh, *J. Alloys Compd.*, 2009, 477,677.
30. H. Smaoui, L. E. L. Mir, H. Guermazi, S. Agnel and A. Toureille,*J. Alloys Compd.*, 2009, 477, 316.
31. A. Gemant, *J. Appl. Phys.*, 1938, 9, 730.
32. A. J. Curtis, *J. Chem. Phys.*, 1962, 36, 3500.
33. G. E. Conklin, *J. Appl. Phys.*, 1964, 35, 3228.
34. M. G. Todd and F. G. Shi, *IEEE Trans. Comp. Packag. Technol.*, 2003, 26, 667.
35. D. H. Kuo, C. C. Chang, T. Y. Su, W. K. Wang and B. Y. Lin, *J. Eur. Ceram. Soc.*, 2001, 21,7.
36. K. Lichtenecker, *Physik,* Z, 1926, 27, 115.
37. M. Carvalho Araújo, C.M. Costa and S. Lanceros Méndez, *J. Non-Cryst. Solids*,2014, 387, 6.
38. A. H. Sihvola and J. A. Kong,*IEEE Trans. Geosci. Remote Sensing*, 1988, 26, 420.
39. Y. Sun, Z. Zhang and C. P. Wong,*Polymer*, 2005, 46, 2297.
40. Y. Rao, J. Qu, T. Marinis and C. P. Wong, *IEEE Trans. Comp. Packag. Technol.*, 2000, 23, 680.
41. D. H. Kuo, C. C. Chang, T. Y. Su, W. K. Wang, B. Y. Lin, *Mater. Chem. Phys.*, 2004, 85, 201.
42. D. W. Richerson, *Modern ceramic engineering: properties processing and use in design*, Taylor and Francis, CRC Press, London, 2006.
43. N. Rajlakshmi, D. P. Tarkes, S. Alok, *Comp. Mater. Sci.*, 2010, 48, 576.
44. R. C. Progelhof, J. L. Throne, R. R. Ruetsch, *Polym. Eng. Sci*., 1976, 16, 615.
45. A. Eucken, *Forschung Gabiete Ingenieur*, 1940, 11, 6.
46. J. C. Maxwell, A Treatise on Electricity and Magnetism. (3rd ed). New York, Dover Publications Inc., 1954.
47. Z. Guocheng, K. Dana, W. Yan, M. Jiri, B. M. Funda, *AUTEX Research Journal*, 2014, 14, 14.
48. Y. Agari, A. Ueda, S. Nagai,*J. Appl. Polym. Sci.*, 1991, 43, 1117.
49. Y. Agari, A. Ueda, S. Nagai,*J. Appl. Polym. Sci.*, 1993, 49, 1625.
50. G. T. N. Tsao, *Industrial & Engineering Chemistry*, 1961, 53, 395.
51. W. Kim, J. W. Bae, D. Choi, S. K. Yong, *Polym. Eng. Sci.,* 1999, 39, 756.
52. R. Hill and P. H. Supancic, *J. Am. Ceram. Soc.*, 2002, 85, 851.
53. L. Holliday and D. Robinson, *J. Mater. Sci.*,1973, 8, 301.
54. R. S. Raghava, *Polym. Compos.*, 1988, 9, 1.
55. P. Patnaik, *Handbook of inorganic chemicals*. McGraw-Hill Professional. p. 1002, 2002.
56. M. Rusu, N. Sofian, D. Rusu, *Polym. Test.* 2001, 20, 409.
57. K. P. Murali, S. Rajesh, O. Prakash, A. R. Kulkarni, R. Ratheesh, *Composites. Part A*, 2009, 40, 1179.
58. A. B. Constantine, *Antenna theory and analysis and design*, 3rd Edition, John Wiley and Sons, Canada, 2005.
59. J. G. Yook, L. Katehi, *IEEE Trans. Antennas Propag.,* 2001, 49, 1282.
60. G. Kumar, K. P. Ray, *Broadband Microstrip Antennas*, Norwood, MA, Artech House, 1996.
61. D. R. Jackson, J. T. Williams, A. K. Bhattacharyya, R. L. Smith, S. J. Buchheit, S. A. Long, *IEEE Trans. Antennas Propag.* 1993, 41, 1026.
62. N. G. Alexopoulos, D. R. Jackson, *IEEE Trans. Antennas Propag.,* 1984, AP-32, 807.
63. J. Varghese, M. Présumey and M. T. Sebastian, K. P. Surendran, *Mater. Chem. Phys.*, 2014, 148, 96.
64. J. Varghese, S. Gopinath and M. T. Sebastian, *Mater. Chem. Phys.*, 2013, 137, 811.